Phase diagram of the ionic Hubbard model with density-dependent hopping

P. Roura-Bas
Centro Atómico Bariloche, GAIDI, CONICET, 8400 Bariloche, Argentina

A. A. Aligia
Instituto de Nanociencia y Nanotecnología CNEA-CONICET, GAIDI, Centro Atómico Bariloche and Instituto Balseiro, 8400 Bariloche, Argentina

(Received 19 April 2023; revised 21 August 2023; accepted 5 September 2023; published 15 September 2023)

We obtain the quantum phase diagram of the ionic Hubbard model including electron-hole symmetric density-dependent hopping. The boundaries of the phases are determined by crossings of excited levels with particular discrete symmetries, which coincide with jumps of charge and spin Berry phases with a topological meaning. Reducing the magnitude of the hopping terms that do not change the total number of singly occupied sites with respect to the other one, the region of the phase diagram occupied by the fully gapped spontaneously dimerized insulator (which separates the band insulating and Mott insulating phases) is enlarged, particularly for small values of the alternating on-site energy. This result might be relevant for experiments in cold atoms in which topological charge pumping is observed when alternation in the hopping is included.

DOI: 10.1103/PhysRevB.108.115132

I. INTRODUCTION

Ultracold quantum gases provide a versatile platform as universal quantum simulators of many-body problems [1]. Cold atoms as well as other platforms have been used to study quantized topological charge pumping in driven systems [2]. A time-dependent adiabatic evolution in a closed cycle in a certain space of parameters constitutes a Thouless pump, in which a quantized amount of charge or spin is transported, which is topologically protected [3,4]. The study of Thouless pumps combines various exciting aspects of modern physics, including topological phases, quantum mechanics, metrology [5], and quantum information processing.

Simulating the noninteracting Rice-Mele model [6] with ultracold atoms, quantized charge pumping has been achieved for bosons [7] and fermions [8]. For the fermionic interacting Rice-Mele model, charge pumping has also been studied theoretically [9] using a pump cycle centered at the origin of a two-dimensional parameter space [(δ, Δ) explained in Sec. II]. In the case of weak enough interaction, the pump cycle encloses two symmetrically located singularities resulting in a pumping of two charges, one for each spin. Notably, the interaction induces an effective repulsion of the singularities while keeping their positions symmetrically disposed. As a consequence, increasing the interaction results in a movement of the singularities towards the frontier of the closed path and when a critical value of the interaction is reached, they are expelled outside from it leading to an abrupt decrease of the quantized charge pumped per cycle from two to zero. This behavior has been recently experimentally observed in an optical lattice [10].

The interacting version of the model (described in detail in Sec. II) is particularly interesting because it also permits the transport of one single charge in the cycle. This has been explored theoretically (including also spin pumping) [11]. To pump one charge per cycle, a closed path is chosen with its center outside the origin of the parameter space and enclosing one singularity in the trajectory. Therefore, the interaction is used to split the degeneracy of the singularities at the origin in the noninteracting model and permits one to select only one of both inside the loop. Remarkably, this half of the usual Thouless pumping has been recently achieved in a dynamical superlattice of fermionic atoms [12].

A feature of the phase diagram for interacting fermionic models is that it includes regions of the parameter space in which the spin gap vanishes. If in an experimental setup the closed path traverses the spin gapless region, the adiabatic charge pumping results in a challenge for the experiment, because traversing a gapless region with finite velocity necessarily induces transitions from the ground state to excited states.

The goal of this work is to study to what extent the region of the phase diagram occupied by the fully gapped phase can be enlarged. To do so, we study the ionic Hubbard model (IHM), which is a general prototype for the interacting Rice-Mele one, with a density-dependent hopping (DDH). In order to solve the model, we use the method of crossings of excited energy levels based on conformal field theory [13–17], already used in Ref. [18] for the standard IHM. For this model including DDH, the method also coincides with that of jumps of charge and spin Berry phases used in Ref. [19].

The paper is organized as follows. In Sec. II we explain the model and its different phases as the parameters are changed. Furthermore, we provide a description of the Thouless pump and the different types of cycles in the parameter space. Moreover, this section gives a detailed explanation that motivates the inclusion of DDH for enlarging the spin gapless region of the phase diagram. In Sec. III we briefly explain the method of

crossings of excited energy levels for solving the model. The resulting phase diagram is contained in Sec. IV. Section V contains a summary and discussion.

II. MODEL AND THOULESS PUMP

The interacting Rice-Mele model including density-dependent hopping has the form

$$H = \sum_{j\sigma}[-1+\delta\,(-1)^j](c^\dagger_{j\sigma}c_{j+1\sigma} + \text{H.c.}) \times [t_{AA}(1-n_{j\bar\sigma})(1-n_{j+1\bar\sigma}) + t_{BB}n_{j\bar\sigma}n_{j+1\bar\sigma} + t_{AB}(n_{j\bar\sigma}+n_{j+1\bar\sigma}-2n_{j\bar\sigma}n_{j+1\bar\sigma})] + \Delta\sum_{j\sigma}(-1)^j n_{j\sigma} + U\sum_j n_{j\uparrow}n_{j\downarrow}. \quad (1)$$

The first term is the DDH, which is alternating for $\delta \neq 0$. The amplitude t_{AA} corresponds to the situation in which only the particle that hops occupies the two nearest-neighbor sites involved in the hopping. For t_{AB} and t_{BB} the total occupancy is 2 and 3, respectively. In the following we assume the electron-hole symmetric case $t_{BB} = t_{AA}$, which is the one implemented experimentally with cold atoms [20–25]. Δ is the alternating on-site energy and U is the on-site Coulomb repulsion. Our conclusions, and our discussions below on the effect of the alternation of the hopping δ are the same if δ affects only the hopping part proportional to t_{AB}, and not the other two.

Usually the pump cycles are performed in a two-dimensional space (δ, p) in which both δ and another parameter p (like Δ or U) depend on time and return to the original value after the cycle. Ideally, in a Thouless pump, a critical point of degeneracy (a singularity) is surrounded in an adiabatic time cycle without closing a gap. In the adiabatic limit, the charge (spin) pumped in the cycle is determined by the evolution of the charge (spin) Berry phase γ_c (γ_s) in the cycle [11].

For the interacting Rice-Mele model for fixed U, the cycles which lead to nontrivial charge pumping enclose at least one of the critical points lying at $\delta = 0$ and $\Delta = \pm\Delta_c$ (see Fig. 1). For $\delta = 0$, the interacting Rice-Mele model is equivalent to the ionic Hubbard model [18,26–34]. It is known that at $\Delta = \pm\Delta_c$ there is a charge transition in which the topologically protected charge Berry phase jumps between the values 0 and π [18], implying a transport of one charge when a time cycle is performed in the plane (δ, Δ) enclosing one of the points $(0, \pm\Delta_c)$ [11,35].

To get insight into the physics of this charge pumping, consider first the limit $t = t_{\alpha\beta} \to 0$ of the IHM ($\delta = 0$). In this case, clearly for $\Delta > \Delta_c \to U/2$, and the half-filled system of interest, all sites with on-site energies $-\Delta$ are filled and the rest are empty. The occupancies at each site are therefore 2020... . This corresponds to the band insulating (BI) phase of the IHM and has a charge Berry phase $\gamma_c = 0\,\text{mod}(2\pi)$ [18]. In fact in the limit $t \to 0$, $\gamma_c = 0$ coincides with the phase of the ground-state expectation value of $\exp[i(2\pi/L)\Sigma_j x_j n_j]$, where n_j is the total occupancy at site j and x_j is the position of this site fixing $x_1 = 0$ [35]. By an elementary calculation, this phase is seen to correspond to 0 mod(2π).

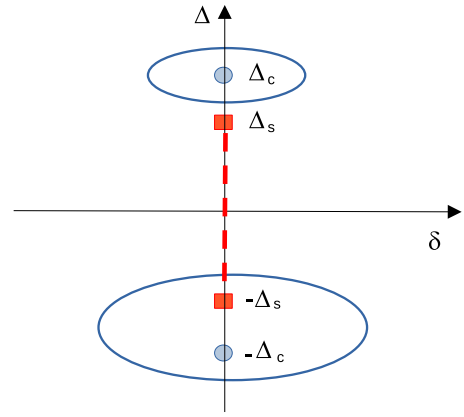

FIG. 1. Scheme of two pump cycles that enclose the charge critical points at $\Delta = \pm\Delta_c$. The spin critical points at $\Delta = \pm\Delta_s$ are also shown. In the segment $\delta = 0$, $-\Delta_s \leqslant \Delta \leqslant \Delta_s$ (dashed line), the spin gap vanishes.

Similarly, for $\Delta < \Delta_c$ the charge distribution is 1111..., with $\gamma_c = \pi$ mod(2π), which corresponds to the Mott insulating (MI) phase. According to the modern theory of polarization, this change of Berry phase corresponds to the transfer of one charge of half a unit cell [11,35]. For finite t, a narrow region of a spontaneously dimerized insulator (SDI) with $\gamma_c = \pi$ appears between the BI and MI phases [18]. In this phase, the probability of finding nearest-neighbor singlets is different in odd and even bonds in the thermodynamic limit, due to a spontaneous breaking of inversion symmetry in this limit [26,29,36,37]. Since at $\delta = 0$, γ_c is protected by inversion symmetry, the charge transition between the BI and SDI phases persists at finite t.

For $\delta \neq 0$, inversion symmetry is lost and γ_c varies continuously. This allows quantized charge pumping of one charge if a circuit like one of those shown in Fig. 1 is followed [11]. For example, taking the circuit at the bottom, beginning at $\delta = 0$ and $\Delta < -\Delta_c$, the system is in the BI phase with $\gamma_c = 0$. Increasing δ, hopping from the odd doubly occupied sites to the even empty sites at their right (larger j and x_j) are favored and γ_c increases. Continuing the circuit increasing Δ and decreasing δ, the topmost point with $\delta = 0$ and $\Delta > -\Delta_c$ is reached (MI phase since also $\Delta > -\Delta_s$) at which the charge distribution is homogeneous and $\gamma_c = \pi$. Continuing the cycle decreasing δ again hopping to the right is favored, this time from the even sites to the odd ones, increasing further γ_c until finally reaching the initial point with $\gamma_c = 2\pi$. Therefore γ_c changed continuously in the cycle from 0 to 2π, which corresponds to a transfer of one electron one unit cell to the right.

At $\Delta = \pm\Delta_s$ there is a spin transition in the IHM ($\delta = 0$) with a jump in the spin Berry phase and a closing of the spin gap for $|\Delta| \leqslant \Delta_s < \Delta_c$ which signals the transition between the SDI and the MI phase. The phase diagram (which is symmetric by a change of sign in Δ) has been constructed in Ref. [18] using the method of crossings of excited energy levels based on conformal field theory [13–17]. The spin gap opens as $|\delta|^{2/3}$ leading to a dimerized phase for finite δ [11].

As was mentioned in Sec. I, if the spin gap vanishes, the adiabaticity of the evolution along the cycle is lost. A cycle

in the plane δ, Δ that encloses a critical point $\Delta = \pm\Delta_c$ and passes far from it, necessarily traverses the MI phase, because Δ_c and Δ_s are very near each other. This case is illustrated at the bottom of Fig. 1. Traversing with a finite velocity, a gapless point produces spin excitations at finite energy, which in turn lead to charge excitations because of the mixing of both sectors at finite energy [26,28]. This leads to oscillations in the charge pumping and loss of quantization with the number of cycles as determined theoretically [11] and experimentally [12]. While the addition of a staggered magnetic field or Ising spin interactions leads to opening of the spin gap and robust charge pumping [11], these terms are not experimentally feasible at present.

Another possibility is to enlarge the region of the SDI phase, separating Δ_c and Δ_s and performing a pump cycle that avoids the MI phase leading to a fully gapped trajectory in the whole cycle, as shown at the top of Fig. 1. This is in principle possible adding the density-dependent hopping. Such a term in an electron-hole symmetric form has been realized in cold atoms using Floquet engineering [20–25]. The Hubbard model with nearest-neighbor hopping dependent on the occupancy of the sites involved (also called correlated hopping) has been derived and studied as an effective model for the superconducting cuprates [38–40], which leads to enhancement of superconductivity for certain parameters [41–44]. Some studies also include nearest-neighbor repulsion [45,46]. In one dimension, phases with dominating singlet-superconducting correlations appear for some parameters [47–50]. At half filling, it has been found that when the hopping term that changes the number of singly occupied sites [t_{AB} in Eq. (1)] is larger than the other two, a dimerized phase with a spin gap is favored [13,19,51,52], which is the desired effect.

In conclusion, the critical points of the pump cycles at which the Berry phases jump lie on the line $\delta = 0$, because for $\delta = 0$, the system has inversion symmetry at each site and as a consequence, the Berry phases can only be either 0 or π (mod 2π). In other words, γ_c/π and γ_s/π become topological numbers protected by inversion symmetry [35]. In addition, the MI phase in which the spin gap vanishes is also restricted to $\delta = 0$. Then to identify a possible cycle that encloses the charge critical point with a ground state separated from the rest of the spectrum in the whole cycle, one can keep $\delta = 0$, where all ground-state degeneracies lay. This is what we do in the rest of the work.

III. METHOD OF CROSSINGS OF EXCITED ENERGY LEVELS

The model in Eq. (1) for $\delta = 0$ becomes the IHM with electron-hole symmetric DDH. It is interesting to note that the standard IHM (without DDH) is integrable according to numerical studies [33] and in fact it can be solved by Bethe ansatz in some cases [34]. A model with only DDH with $\Delta = 0$ can also be solved exactly using the Bethe ansatz for particular parameters [53].

In this work, in order to calculate the phase diagram of the model we use the method of crossings of excited energy levels [13–17]. In one dimension, the dominant correlations at large distances determine the thermodynamic phase of the system. In usual cases in which there is no long-range order, one expects that residual interactions between chains gives rise to this order according to the prevailing long-distance behavior. The idea of the method is that the dominant correlations at large distances correspond to the smallest excitation energies. The crossings of excited levels in appropriate symmetry sectors therefore correspond to phase transitions. The method has been used before for similar models [13,18,19]. For our model, this method and the jumps in the values of the Berry phases give the same information [18], but the crossings of appropriate energy levels is simpler and requires less computational cost.

In terms of jumps in Berry phases, the method can be understood as follows. As explained in the previous section, these jumps correspond to changes in the topological sector of the model which are relevant for charge and spin pumping. The charge Berry phase is the phase accumulated by the ground state, using twisted boundary conditions in which the hopping term at one bond only, is changed by a factor $e^{i\Phi}$, as Φ varies from 0 to 2π. For the spin Berry phase the factor is $e^{i\Phi}$ for spin up, and $e^{-i\Phi}$ for spin down [35]. During the cycle, for an even number of sites L, the ground-state energy is minimized when $\Phi = \pi$ (antiperiodic boundary conditions) if L is a multiple of 4, and $\Phi = 0$ (periodic boundary conditions) for L even but not a multiple of 4. These boundary conditions are known as closed-shell conditions. The opposite case corresponds to open-shell boundary conditions at which the ground state has a maximum as a function of Φ. A jump in any or both Berry phases takes place at parameters for which at this maximum, the ground state becomes degenerate with an excited state with opposite value of the Berry phase [18]. Our method is essentially to identify these crossings separating both states by their properties under discrete symmetries of the model at the specific value of Φ where the crossing occurs.

The crossings for both charge and spin transitions are determined using open-shell boundary conditions. The charge transition is determined by a crossing in the ground state of the two singlets of lowest energy with opposite parity under inversion. In the BI phase the ground state is even under inversion, while it is odd in the other two phases. The spin transition between SDI and MI phases, is determined by the crossing of the excited even singlet with lowest energy and the lowest excited odd triplet, which has less energy in the MI phase. In the actual calculation we have not evaluated the total spin S of the states, but used the parity under time reversal (the singlet is even and the triplet with total spin projection $S_z = 0$ is odd). All these states have wave vector 0 for $\Delta \neq 0$.

The method is expected to be very accurate. In particular, for the model with only DDH and on-site repulsion U [Eq. (1) with $\Delta = \delta = 0$], the phase diagram obtained from jumps in the Berry phases practically coincides with that obtained from bosonization at several densities for small values of U, for which bosonization is expected to be quantitatively valid [52].

To determine the phase diagram we have set $t_{AB} = 1$ as the unit of energy. Then for a given value of t_{AA} and Δ we have calculated the values of U that correspond to the charge (U_c) and spin (U_s) transitions using the method of crossings of energy levels for all even number of sites L in the range $6 \leqslant L \leqslant 14$. The results were extrapolated to $L \to \infty$ using a quadratic polynomial in $1/L$. Examples of the extrapolation are shown

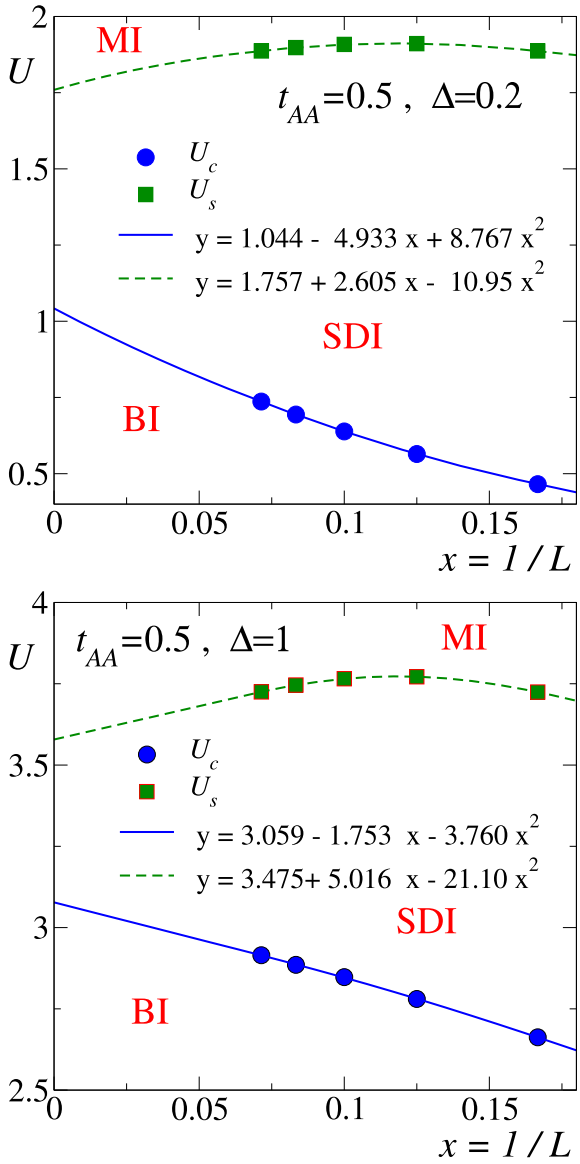

FIG. 2. Critical values of U for the charge and spin transitions for $t_{AB} = 1$, and other parameters indicated inside each figure.

in Fig. 2. The curves fit the data well and the finite-size effects are in general small, except for the charge transition for small values of Δ. In any case, a deviation of the value of U_c for $\Delta = 0.2$ for up to 20% is very unlikely from the trend of the curve and does not modify our conclusions. Calculations with $L = 16$ are possible, but they are very time-consuming and lead to a modification of the extrapolated values of U_c by less than 1% in the region of interest of small Δ.

IV. RESULTS

In Fig. 3, we compare the phase diagram of the standard IHM with that in which the hopping terms that do not alter the total number of singly occupied sites $t_{AA} = t_{BB}$ is reduced. For fixed Δ the system is a BI for low U and a MI for large U. Both phases are separated by a narrow region of the SDI phase. Increasing U, the charge transition at $U = U_c$ (with a jump in γ_c from 0 to π [18]) corresponds to the change from

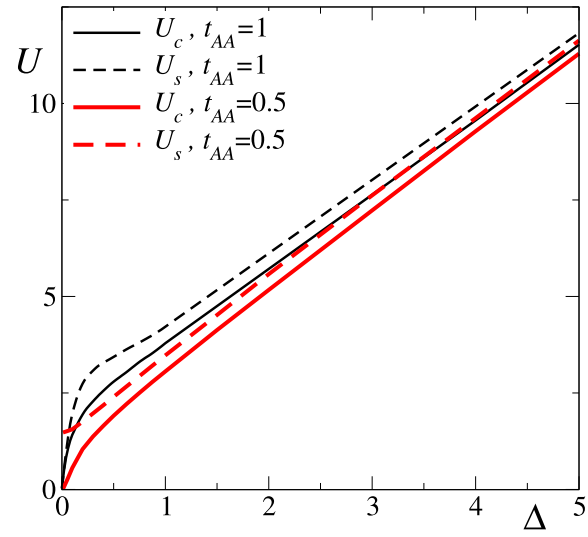

FIG. 3. Phase diagram of the IHM with DDH in the Δ, U plane for $t_{AB} = 1$, and two values of $t_{AA} = t_{BB}$. The region between the full and dashed lines corresponds to the SDI.

the BI to the SDI, and at the spin transition for $U = U_s$ (with a jump in γ_c from 0 to π [18]) the SDI changes to the MI.

For $\Delta \gtrsim 3t_{AB}$ the width of the SDI phase is of the order of a fraction of t_{AB}. Naturally, keeping the three hopping terms equal $t_{\alpha\beta} = t$ and reducing t, the SDI phase shrinks and both $U_c, U_s \to 2\Delta$ for $t \to 0$. It is therefore noticeable that reducing only $t_{AA} = t_{BB}$, the extension of the SDI phase is *increased* for $\Delta > 3t_{AB}$ and by about 15% for $\Delta = 5t_{AB}$.

As is apparent in Fig. 4, this effect is more dramatic for $\Delta < 0.2t_{AB}$. In fact, contrary to the case of equal $t_{\alpha\beta} = t$, there is a finite spin gap for small U even at $\Delta = 0$ when $t_{AB} > t_{AA} = t_{BB}$. This result has been found before [13,19,51,52] and can be understood from analytical calculations using bosonization [51,52] which coincide very well with numerical calculations [19] for small values of U.

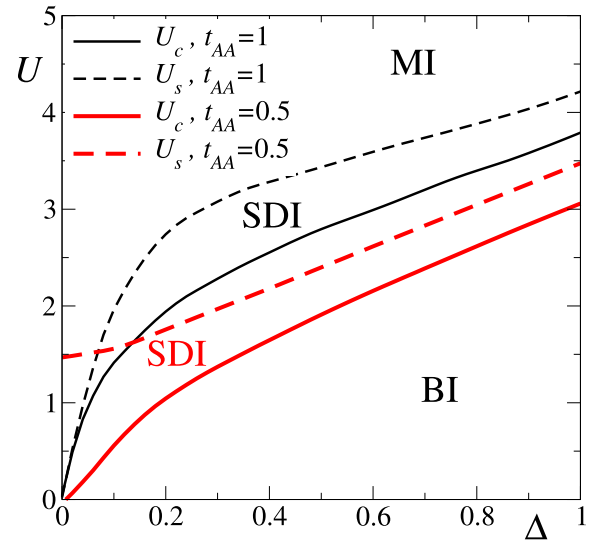

FIG. 4. Same as Fig. 3 in a smaller region of Δ.

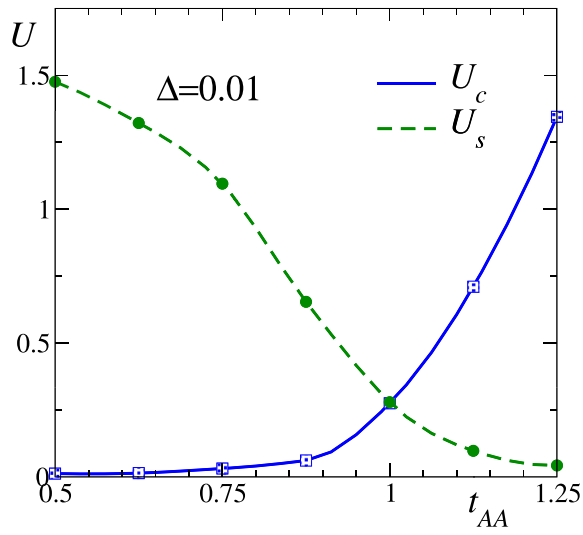

FIG. 5. Critical values of U at the charge and spin transitions as a function of $t_{AA} = t_{BB} =$ for $t_{AB} = 1$ and $\Delta = 0.01$.

The particular features of the phase diagram for small Δ, render it possible to perform time evolutions around a critical point for the charge transition that transport a quantized unit of charge per cycle with open charge and spin gaps in the whole cycle, like the pump cycle shown at the top of Fig. 1. For example for $\Delta = 0.2$, $t_{AB} = 1$, and $t_{AA} = t_{BB} = 0.5$, we find $U_c = 1.044$ and $U_s = 1.757$. Performing a time-dependent cycle in either plane (δ, Δ) or (δ, U) with the center at the charge critical point (with $\delta = 0$) and the amplitude in Δ of about ± 0.2 or in U near ± 0.5, the cycle never reaches the MI phase and therefore, the spin gap is always open. One point that should be taken into account is that the spin transition is of the Kosterlitz-Thouless type, and therefore the spin gap is exponentially small in the SDI phase near the transition boundary [19]. Therefore it might be convenient to move the time cycle away from the MI-SDI boundary, keeping the critical point inside the cycle.

In the previous figures we have taken $t_{AA} = t_{BB} = t_{AB}/2$. In Fig. 5 we show how the values of U at both transitions change with $t_{AA} = t_{BB}$ for a small value of Δ. We can see that the change is more rapid for t_{AA} near t_{AB} and the increase in U_s is already large for $t_{AA}/t_{AB} = 3/4$.

When t_{AA}/t_{AB} exceeds 1 for a significant amount, U_c becomes larger than U_s giving rise to a new phase in between. A detailed study of the properties of this phase is beyond the scope of the present work. For $\Delta = 0$, studies with bosonization indicate that this region corresponds to a Tomonaga-Luttinger liquid (gapless) phase with triplet superconducting and bond spin-density wave correlations dominating at large distances [19,51,52]. However, Δ is a relevant perturbation that can substantially modify the physics. In principle, a long-range charge-density wave is expected that opens a charge gap. However, numerical studies in the model with $\Delta = 0$ but adding nearest-neighbor repulsion V, which also favors a charge-density wave, indicate that the charge gap still vanishes for small values of V [46].

V. SUMMARY AND DISCUSSION

We have calculated the quantum phase diagram of the ionic Hubbard model, including electron-hole symmetric density-dependent hopping, which corresponds to Eq. (1) with $\delta = 0$ and $t_{AA} = t_{BB} < t_{AB}$, using the method of crossings of excited energy levels in rings of up to 14 sites.

The model has three phases: the BI, the MI, and a narrow region of the SDI in between. The BI and SDI are fully gapped except at the transition points between them at $\Delta = \pm\Delta_c$, which lead to topological singularities at the points $(0, \pm\Delta_c)$ in the two-dimensional space (δ, Δ). Therefore an adiabatic cycle in this space which encloses one of these singularities leads to a Thouless pumping of one charge per cycle.

Nevertheless, since the region of the SDI is very narrow, experimental pump cycles with cold atoms that surround only one of the charge critical points, for which quantized pumping is observed, usually cross the MI region in which the spin gap is closed, leading to transition to excited states and loss of adiabaticity and quantized charge transport after the first pump cycle [12].

We obtain that a reduction of $t_{AA} = t_{BB}$ with respect to t_{AB}, increases the region of the phase diagram occupied by the fully gapped SDI phase, particularly for $|\Delta| < t_{AB}$ and $U < 2t_{AB}$. This result is of possible relevance to experiments similar to the above mentioned. Floquet engineering renders it possible to achieve the region $t_{AA} = t_{BB} < t_{AB}$ [20–25]. and therefore enlarge the region of the gapped SDI phase.

To confirm the possibilities of this proposal, it would be useful to calculate the spin gap and the internal charge gap between even and odd singlets in the SDI phase. This would require a study of longer chains using, for example, density-matrix renormalization group. It would also be useful to simulate the time dependence in pumping cycles similar to the ones suggested here, using infinite time-evolving block decimation.

ACKNOWLEDGMENTS

We thank Konrad Viebahn, Eric Bertok, and Fabian Heidrich-Meisner for useful discussions. A.A.A. acknowledges financial support provided by PICT 2017-2726 and PICT 2018-01546 of the ANPCyT, Argentina.

[1] G. Gross and I. Bloch, Quantum simulations with ultracold atoms in optical lattices, Science **357**, 995 (2017).

[2] R. Citro and M. Aidelsburger, Thouless pumping and topology, Nat. Rev. Phys. **5**, 87 (2023).

[3] D. J. Thouless, Quantization of particle transport, Phys. Rev. B **27**, 6083 (1983).

[4] Q. Niu and D. J. Thouless, Quantised adiabatic charge transport in the presence of substrate disorder and many-body interaction, J. Phys. A: Math. Gen. **17**, 2453 (1984).

[5] J. P. Pekola, O.-P. Saira, V. F. Maisi, A. Kemppinen, M. Möttönen, Y. A. Pashkin, and D. V. Averin, Single-electron current sources: Toward a refined definition of the ampere, Rev. Mod. Phys. **85**, 1421 (2013).

[6] M. J. Rice and E. J. Mele, Elementary Excitations of a Linearly Conjugated Diatomic Polymer, Phys. Rev. Lett. **49**, 1455 (1982).

[7] S. Nakajima, T. Tomita, S. Taie, T. Ichinose, H. Ozawa, L. Wang, M. Troyer, and Y. Takahashi, Topological Thouless pumping of ultracold fermions, Nat. Phys. **12**, 296 (2016).

[8] M. Lohse, C. Schweizer, O. Zilberberg, M. Aidelsburger, and I. Bloch, A Thouless quantum pump with ultracold bosonic atoms in an optical superlattice, Nat. Phys. **12**, 350 (2016).

[9] M. Nakagawa, T. Yoshida, R. Peters, and N. Kawakami, Breakdown of topological Thouless pumping in the strongly interacting regime, Phys. Rev. B **98**, 115147 (2018).

[10] A.-S. Walter, Z. Zhu, M. Gächter, J. Minguzzi, S. Roschinski, K. Sandholzer, K. Viebahn, and T. Esslinger, Quantisation and its breakdown in a Hubbard-Thouless pump, Nat. Phys. (2023), doi:10.1038/s41567-023-02145-w.

[11] E. Bertok, F. Heidrich-Meisner, and A. A. Aligia, Splitting of topological charge pumping in an interacting two-component fermionic Rice-Mele Hubbard model, Phys. Rev. B **106**, 045141 (2022).

[12] K. Viebahn, A.-S. Walter, E. Bertok, Z. Zhu, M. Gächter, A. A. Aligia, F. Heidrich-Meisner, and T. Esslinger, Interaction-induced charge pumping in a topological many-body system, arXiv:2308.03756.

[13] M. Nakamura, Tricritical behavior in the extended Hubbard chains, Phys. Rev. B **61**, 16377 (2000).

[14] K. Nomura and K. Okamoto, Critical properties of S=1/2 antiferromagnetic XXZ chain with next-nearest-neighbour interactions, J. Phys. A: Math. Gen. **27**, 5773 (1994).

[15] M. Nakamura, K. Nomura, and A. Kitazawa, Renormalization Group Analysis of the Spin-Gap Phase in the One-Dimensional *t-J* Model, Phys. Rev. Lett. **79**, 3214 (1997).

[16] M. Nakamura, Mechanism of CDW-SDW transition in one dimension, J. Phys. Soc. Jpn. **68**, 3123 (1999).

[17] R. D. Somma and A. A. Aligia, Phase diagram of the *XXZ* chain with next-nearest-neighbor interactions, Phys. Rev. B **64**, 024410 (2001).

[18] M. E. Torio, A. A. Aligia, and H. A. Ceccatto, Phase diagram of the Hubbard chain with two atoms per cell, Phys. Rev. B **64**, 121105(R) (2001).

[19] A. A. Aligia, K. Hallberg, C. D. Batista, and G. Ortiz, Phase diagrams from topological transitions: The Hubbard chain with correlated hopping, Phys. Rev. B **61**, 7883 (2000).

[20] R. Ma, M. E. Tai, P. M. Preiss, W. S. Bakr, J. Simon, and M. Greiner, Photon-Assisted Tunneling in a Biased Strongly Correlated Bose Gas, Phys. Rev. Lett. **107**, 095301 (2011).

[21] F. Meinert, M. J. Mark, K. Lauber, A. J. Daley, and H.-C. Nägerl, Floquet Engineering of Correlated Tunneling in the Bose-Hubbard Model with Ultracold Atoms, Phys. Rev. Lett. **116**, 205301 (2016).

[22] R. Desbuquois, M. Messer, F. Görg, K. Sandholzer, G. Jotzu, and T. Esslinger, Controlling the Floquet state population and observing micromotion in a periodically driven two-body quantum system, Phys. Rev. A **96**, 053602 (2017).

[23] F. Görg, M. Messer, K. Sandholzer, G. Jotzu, R. Desbuquois, and Tilman Esslinger, Enhancement and sign change of magnetic correlations in a driven quantum many-body system, Nature (London) **553**, 481 (2018).

[24] M. Messer, K. Sandholzer, F. Görg, J. Minguzzi, R. Desbuquois, and T. Esslinger, Floquet Dynamics in Driven Fermi-Hubbard Systems, Phys. Rev. Lett. **121**, 233603 (2018)

[25] F. Görg, K. Sandholzer, J. Minguzzi, R. Desbuquois, M. Messer, and T. Esslinger, Realization of density-dependent Peierls phases to engineer quantized gauge fields coupled to ultracold matter, Nat. Phys. **15**, 1161 (2019).

[26] M. Fabrizio, A. O. Gogolin, and A. A. Nersesyan, From Band Insulator to Mott Insulator in One Dimension, Phys. Rev. Lett. **83**, 2014 (1999).

[27] S. R. Manmana, V. Meden, R. M. Noack, and K. Schönhammer, Quantum critical behavior of the one-dimensional ionic Hubbard model, Phys. Rev. B **70**, 155115 (2004).

[28] A. A. Aligia, Charge dynamics in the Mott insulating phase of the ionic Hubbard model, Phys. Rev. B **69**, 041101(R) (2004).

[29] C. D. Batista and A. A. Aligia, Exact Bond Ordered Ground State for the Transition between the Band and the Mott Insulator, Phys. Rev. Lett. **92**, 246405 (2004).

[30] L. Tincani, R. M. Noack, and D. Baeriswyl, Critical properties of the band-insulator-to-Mott-insulator transition in the strong-coupling limit of the ionic Hubbard model, Phys. Rev. B **79**, 165109 (2009).

[31] M. E. Torio, A. A. Aligia, G. I. Japaridze, and B. Normand, Quantum phase diagram of the generalized ionic Hubbard model for AB_n chains, Phys. Rev. B **73**, 115109 (2006).

[32] L. Stenzel, A. L. C. Hayward, C. Hubig, U. Schollwöck, and F. Heidrich-Meisner, Quantum phases and topological properties of interacting fermions in one-dimensional superlattices, Phys. Rev. A **99**, 053614 (2019).

[33] A. Hosseinzadeh and S. A. Jafari, Quantum integrability of 1D ionic Hubbard model, Ann. Phys. **532**, 1900601 (2020).

[34] A. Hosseinzadeh and S. A. Jafari, Generalization of Lieb-Wu wave function inspired by one-dimensional ionic Hubbard model, Ann. Phys. **414**, 168075 (2020).

[35] A. A. Aligia, Topological invariants based on generalized position operators and application to the interacting Rice-Mele model, Phys. Rev. B **107**, 075153 (2023).

[36] M. Fabrizio, A. O. Gogolin, and A. A. Nersesyan, Critical properties of the double-frequency sine-Gordon model with applications, Nucl. Phys. B **580**, 647 (2000).

[37] A. A. Aligia and C. D. Batista, Dimerized phase of ionic Hubbard models, Phys. Rev. B **71**, 125110 (2005).

[38] H. B. Schüttler and A. J. Fedro, Copper-oxygen charge excitations and the effective-single-band theory of cuprate superconductors, Phys. Rev. B **45**, 7588 (1992).

[39] M. E. Simon, M. Baliña, and A. A. Aligia, Effective one-band hamiltonian for cuprate superconductor metal-insulator transition, Phys. C (Amsterdam, Neth.) **206**, 297 (1993).

[40] M. E. Simon and A. A. Aligia, Brinkman-Rice transition in layered perovskites, Phys. Rev. B **48**, 7471 (1993).

[41] J. Hirsch, Bond-charge repulsion and hole superconductivity, Phys. C (Amsterdam, Neth.) **158**, 326 (1989).

[42] J. E. Hirsch and F. Marsiglio, Hole superconductivity: Review and some new results, Phys. C (Amsterdam, Neth.) **162-164**, 591 (1989).

[43] L. Arrachea and A. A. Aligia, Pairing correlations in a generalized Hubbard model for the cuprates, Phys. Rev. B **61**, 9686 (2000).

[44] S. Jiang, D. J. Scalapino, and S. R. White, A single-band model with enhanced pairing from DMRG-based downfolding of the three-band Hubbard model, arXiv:2303.00756.

[45] A. A. Aligia, L. Arrachea, and E. R. Gagliano, Phase diagram of an extended Hubbard model with correlated hopping at half filling, Phys. Rev. B **51**, 13774 (1995).

[46] L. Arrachea, E. Gagliano, and A. A. Aligia, Ground-state phase diagram of an extended Hubbard chain with correlated hopping at half-filling, Phys. Rev. B **55**, 1173 (1997).

[47] A. A. Aligia, A. Anfossi, L. Arrachea, C. Degli Esposti Boschi, A. O. Dobry, C. Gazza, A. Montorsi, F. Ortolani, and M. E. Torio, Incommmensurability and Unconventional Superconductor to Insulator Transition in the Hubbard Model with Bond-Charge Interaction, Phys. Rev. Lett. **99**, 206401 (2007).

[48] A. O. Dobry and A. A. Aligia, Quantum phase diagram of the half filled Hubbard model with bond-charge interaction, Nucl. Phys. B **843**, 767 (2011).

[49] A. Montorsi, U. Bhattacharya, Daniel González-Cuadra, M. Lewenstein, G. Palumbo, and L. Barbiero, Interacting second-order topological insulators in one-dimensional fermions with correlated hopping, Phys. Rev. B **106**, L241115 (2022).

[50] W. Chen, J. Zhang, and H. Ding, Ground-state instabilities in a Hubbard-type chain with particular correlated hopping at non-half-filling, Results in Phys. **49**, 106472 (2023).

[51] G. I. Japaridze and A. P. Kampf, Weak-coupling phase diagram of the extended Hubbard model with correlated-hopping interaction, Phys. Rev. B **59**, 12822 (1999).

[52] A. A. Aligia and L. Arrachea, Triplet superconductivity in quasi-one-dimensional systems, Phys. Rev. B **60**, 15332 (1999).

[53] I. N. Karnaukhov, Model of Fermions with Correlated Hopping (Integrable Cases), Phys. Rev. Lett. **73**, 1130 (1994).